Theoretical & Applied Mechanics Letters 10 (2020) 366-376

Contents lists available at ScienceDirect

Theoretical & Applied Mechanics Letters

journal homepage: www.elsevier.com/locate/taml

Letter

Constructal design method dealing with stiffened plates and symmetry boundaries

Rodrigo R. Amaral[a], Grégori S. Troina[a], Cristiano Fragassa[b,*], Ana Pavlovic[b], Marcelo L. Cunha[a], Luiz A.O. Rocha[c], Elizaldo D. dos Santos[a], Liércio A. Isoldi[a]

[a] *School of Engineering, Federal University of Rio Grande, Rio Grande, Brazil*
[b] *Advanced Applications in Mechanical Engineering and Materials Technology, University of Bologna, Bologna, Italy*
[c] *Departament of Mechanical Engineering, University of Vale do Rio dos Sinos, São Leopoldo, Brazil*

HIGHLIGHTS

- The mere fact of adding stiffeners does not necessarily imply an improvement in mechanical behavior.
- Constructal design can effectively promote the geometric optimization of stiffened plate.
- Maximum deflection of optimized stiffened plate is 95.23% lower than reference.
- Maximum von Mises stress of optimized stiffened plate is 44.98% lower than reference.
- A processing time reduction of 75% can be reached by the proposed computational model.

ARTICLE INFO

Article history:
Received 20 April 2020
Received in revised form 30 April 2020
Accepted 6 May 2020
Available online 22 May 2020
This article belongs to the Solid Mechanics.

Keywords:
Deflection minimization
Stress minimization
Optimal design
Plates with stiffeners
Bending

ABSTRACT

A new computational procedure for modelling the structural behavior of stiffened plates with symmetry boundary conditions is here presented. It uses two-dimensional finite elements as a way to decrease computational time without losing precision thanks to a relatively small number of elements applied for analyzing out-of-plane displacements (deflections) and stresses. Adding, the constructal design method was included in the procedure, together with the exhaustive search technique, with the scope to optimize the stress/strain status of stiffened plates by design changes. For the purpose, a reference plate without stiffeners was initially design and used as starting point. Part of the volume was reshaped into stiffeners: thickness was reduced maintaining unchanged weight, length and width. The main goal was to minimize strains and stresses by geometric changes. Results demonstrated that, thanks to this design procedure, it is always possible to find an adequate geometry transformation from reference plate into stiffeners, allowing significant improvements in mechanical behavior.

Plates are thin-walled structures that result from the engineering tendency to find a compromise between the high structural load-carrying capacity and low structural weight [1]. Whereas the thin-wallness does a great job in achieving this objective, it also makes the structures more susceptible and sensitive to dynamic loads, buckling, etc. Various engineering solutions have been developed to address this aspect. Some of those imply the use of rather modern materials such as fiber-reinforced composite materials [2, 3] to produce directionally dependent properties, or even the so-called "smart" materials to produce active structural behavior [4]. Those solutions involve significant expenses. On the other hand, one of the most frequently used classical solutions characterized by high robustness, cost-effectiveness and relative simplicity is the application of stiffeners.

* Corresponding author.
E-mail address: cristiano.fragassa@unibo.it (C. Fragassa).

http://dx.doi.org/10.1016/j.taml.2020.01.042

Plates with stiffeners may have a higher strength with a relatively lower amount of material than plates which contain no reinforcement, making them an economical structure because it presents an improvement in the resistance and rigidity in relation to its weight. These structural components mainly use steel as a material for its fabrication due to their high resistance in the different states of stresses. They can be used in architectural engineering, for example, in reinforced concrete slabs with unidirectional or bidirectional beams, often used on the floor of buildings. In civil engineering, decks of road bridges generally consist of stiffened plates with rectangular, triangular, or trapezoidal ribs. Also, the use of stiffened plates is indispensable in naval and aerospace structures: being found in the hull, the deck and the bottom of the ships, as well as in naval superstructures; while the wings and the fuselage of the aircrafts are composed mainly by stiffened plate [5, 6].

According to Salomon [7], different approaches for the analysis of plates with stiffeners can be employed, highlighting the model of orthotropic plate, used mainly in obtaining solutions by analytical means; and the model of plate-stiffening system, widely used in numerical methods. The following researches can be mentioned addressing the behavior of stiffened plates: O'Leary and Harari [8] developed a finite element method (FEM) based procedure for the modeling of thin plates reinforced with thicker and widely spaced stiffeners. Sapountzakis and Katsikadelis [9] presented a stiffened plate analysis that considers the forces and strains in the plane of the plate as well as the axial stresses and strains present in the stiffeners. Banai and Pedatzur [10] developed an algorithm of an orthotropic model for stiffened plates to estimate the maximum deflection caused by a uniformly distributed transverse load. Sapountzakis and Mokos [11] presented a general solution for stiffened plates in their deformed configuration, the analysis of this model considered the nonlinear distribution of the transverse shear force of the interface between the plate and the stiffener, such as the non-uniform torsion of the stiffeners. Bhaskar and Pydah [12] presented an analytical elastic solution for stiffened plates, so that the plate is modeled as a 3D solid and the stiffeners are treated as a plane stress problem due to strain caused by shear force and rotational inertia considered in the analysis. Troina et al. [13] presented a geometric optimization of simply supported stiffened steel plates subjected to transversal load through the construtal design (CD) allied to exhaustive search (ES), with SHELL93 and SOLID95 computational models developed in the ANSYS Mechanical APDL and determined that the redistribution of the material used in the construction of stiffened plates allows a significant improvement in the structural rigidity regarding the central deflection of the plates.

As Troina et al. [13], the present work also associates FEM (by ANSYS Mechanical APDL), CD, and ES for a geometric optimization of stiffened steel plates under bending. Here, however, a new computational model with symmetry boundary conditions is developed; the stiffened plates are considered as clamped; and the minimization of maximum deflection as well maximum von Mises stress are adopted as performance indicators.

According to Bejan and Lorente [14] and Bejan [15, 16] the CD can be defined as the philosophy of evolutionary design for engineering systems, being also called as design with constructal theory (DCT). As explained by Bejan and Lorente [17], the constructal theory is the view that the generation of images of design (pattern, rhythm) in nature is a phenomenon of physics which is covered by a principle: the constructal law of design and evolution in nature. The constructal law states that: for a finite-sized flow system to persist in time (to live), its configuration should evolve such that it facilitates access to its currents (fluid, energy, flow of stresses, species, etc.). The CD application in fluid mechanics and heat transfer flow systems is scientifically enshrined, existing innumerous publication about these subjects. For instance, in fluid mechanics CD is used to determine: the best cross section that minimizes the pressure drop of the flows in ducts [18, 19]; the best configuration of the vascular channels when dealing with turbulent flows [20]. In its turn, in heat transfer CD is adopted to define: the best cooling cavities in conductive solids with uniform heat generation, for C- and T-shaped cavities [21] as well as H- and T-Y shaped cavities [22, 23]. In addition, one can find studies involving a multi-objective problem, e.g. in Ref. [24], where the maximization of Nusselt number and the minimization of the drag coefficient for a mixed convective flow over a triangular arrangement of circular cylinders were concomitantly considered. Despite the enormous spread of CD in these areas, in the structural engineering field there are only few works using this method in literature. It is possible to quote Bejan and Lorente [14], Lorente et al. [25] and Isoldi et al. [26] which stated that it is possible to apply the CD method in structural engineering problems (based on the existing analogy among heat transfer, fluid mechanics and mechanics of materials areas). One can also find the application of the CD for the analysis of aircraft structures in Mardanpour et al. [27] and Izadpanahi et al. [28]. Regarding the research novelty, to the authors' knowledge, no other contribution is currently available, specifically dealing with the employment of CD to stiffened steel plates in such conditions of loads and constraints. However, there are some related studies. Helbig et al. [29] and Da Silva et al. [30] analyzed the elastic and elasto-plastic buckling of simply supported steel plates with centered cutouts; Lima et al. [31, 32] studied the elasto-plastic buckling of simply supported stiffened steel plates; and finally De Queiroz et al. [33] and Troina et al. [13] investigated the bending of simply supported stiffened steel plates.

It is important to highlight that CD is a method for investigation of design based in a physical principle (the constructal law of design and evolution) for deterministic generation of design for any finite flow system [16]. Several optimization methods, since ES until heuristic techniques (as genetic algorithm, simulated annealing, differential evolution and others) can be associated with CD, which is the method for geometric investigation. More important than the achievement of optimal configurations, CD is concerned with the influence of design over system performance. Therefore, we believe that the main contribution of the present work is to show the influence of design (represented by the degrees of freedom and constraints) over the performance of the stiffened plates following a physical principle of design.

Concerning the proposed computational model, it was developed in ANSYS Mechanical APDL (Release 18.2) and employs the finite element SHELL281 (Fig. 1), which is suitable for the analysis of thin-walled shells and plates. The SHELL281 has eight nodes with six degrees of freedom per node (three translations in the x, y, and z axes and three rotations around the x, y, and z axes), being based on the Reissner–Mindlin theory [34].

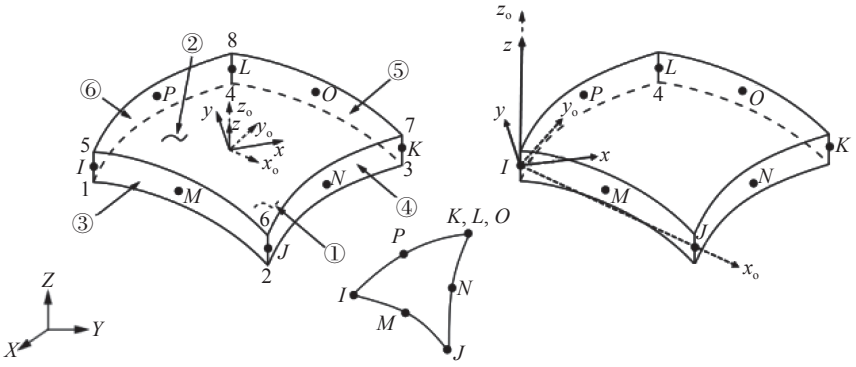

Fig. 1. Finite element SHELL281 [34]

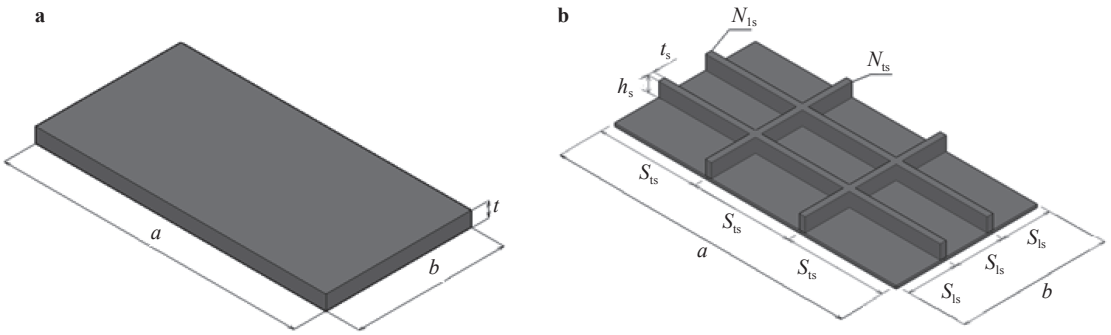

Fig. 2. Constructal design application: **a** reference plate and **b** stiffened plate P(2, 2)

It is important to mention that the developed computational model, unlike most computational models found in the literature for stiffened plates, adopts the symmetry boundary conditions. The use of the symmetry boundary conditions allows the reduction of processing time and the use of a more refined mesh, since it is possible to consider a computational domain with half or a quarter of the problem when it presents symmetry characteristics in relation to its geometry, loading, bonding conditions and material properties. When applying the symmetry boundary conditions it is assumed that the out-of-plane translations and in-plane rotations are set to zero [34].

From the CD application it is possible to define different stiffened plate geometries, composing the search space of the analysis. To do so, a non-stiffened plate (with length a, width b and thickness t) was used as reference. The total steel volume and the dimensions a and b of the reference plate are kept constant, while a fraction of its volume (identified by ϕ) is transformed into stiffeners from the decreasing of its thickness (Fig. 2).

This volumetric fraction is a restriction parameter of the CD method and is defined as:

$$\phi = \frac{V_s}{V_r} = \frac{N_{ls}\,(a h_s t_s) + N_{ts}\,[(b - N_{ts}\,t_s)\,h_s\,t_s]}{abt}, \tag{1}$$

where V_s is the volume of the reference plate transformed into stiffeners, V_r is the total volume of the reference plate, N_{ls} is the number of longitudinal stiffeners, N_{ts} is the number of transverse stiffeners, h_s is the height of the stiffeners and t_s is the thickness of the stiffeners. In addition to the ϕ parameter, N_{ls}, N_{ts}, and ratio h_s/t_s are adopted as degrees of freedom of the CD method, being its variations responsible by the generation of the geometric configurations which compose the search space.

So, the analysis involved plates formed by 25 combinations of longitudinal and transverse stiffeners, obeying the format P(N_{ls}, N_{ts}), varying the following degrees of freedom: N_{ls} = 2, 3, 4, 5, 6 and N_{ts} = 2, 3, 4, 5, 6. In view of this, the following plates were analyzed: P(2, 2), P(2, 3), P(2, 4), P(2, 5), P(2, 6), P(3, 2), P(3, 3), P(3, 4), P(3, 5), P(3, 6), P(4, 2), P(4, 3), P(4, 4), P(4, 5), P(4, 6), P(5, 2), P(5, 3), P(5, 4), P(5, 5), P(5, 6), P(6, 2), P(6, 3), P(6, 4), P(6, 5), and P(6, 6), as illustrated in Fig. 3. Regarding the stiffeners, they have a rectangular cross-section and commercial values of thicknesses of steel plates were adopted (3.18, 4.75, 6.35, 8.00, 9.53, 12.70, 15.90, 19.21, 22.20, and 25.40 mm). Besides, four geometrical constraints are imposed: (1) the height of longitudinal and transverse stiffeners are the same; (2) the height of the stiffeners cannot be greater than 0.3 m, in order to avoid geometric disproportions between the height of the stiffener and the lateral dimensions of the plate; (3) the ratio h_s/t_s must be greater than 1 to prevent the thickness of the stiffener being greater than its height, which would de-characterize the stiffener which must have a height greater than its thickness; (4) as depicted in Fig. 2, the stiffeners have equidistant longitudinal spacing S_{ls} and transverse spacing S_{ts} given, respectively, by

$$S_{ls} = \frac{b}{N_{ls} + 1}, \tag{2}$$

$$S_{ts} = \frac{a}{N_{ts} + 1}. \tag{3}$$

Concerning the reference plate, it is adopted $a = 2$ m, $b = 1$ m, and $t = 20$ mm, being made of structural steel A-36 with elastic modulus of $E = 200$ GPa, Poisson's ratio of $\nu = 0.3$ and yielding strength of $\sigma_y = 250$ MPa [35]. The ratio between the volume of material transformed into stiffeners and the volume of the reference plate is $\phi = 0.3$, i.e., 30% of the total steel volume is used as stiffeners (based on Ref. [13]). The edges of reference plate, as well as of the stiffened plates (including the edges of the stiffeners), are considered as clamped. For all plates a uniformly distributed transverse loading of 10 kPa is taken into account, ensuring a linear-elastic behavior.

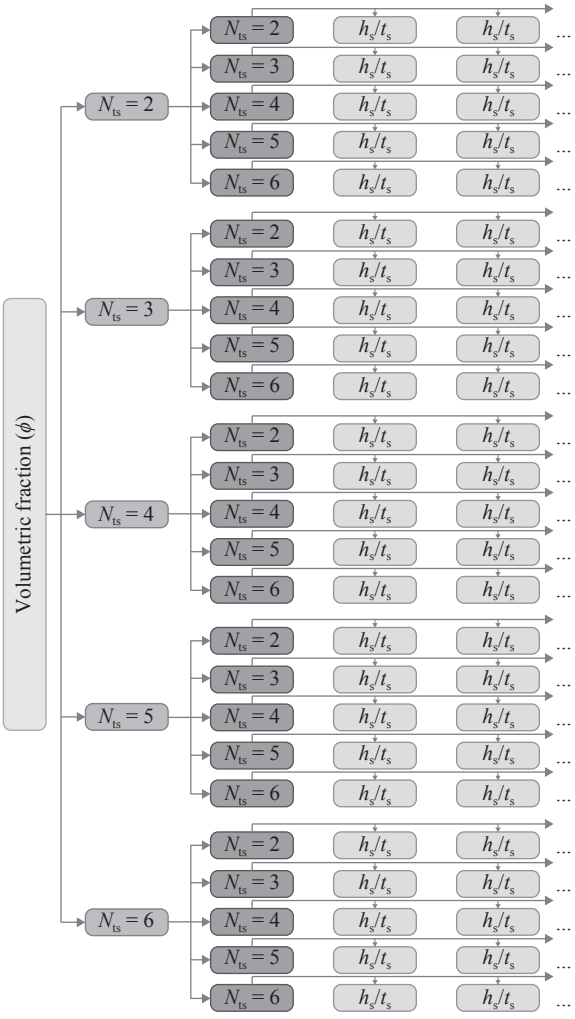

Fig. 3. Geometric onfigurations generated by CD method

Finally, the geometric configurations of the search space are numerically simulated and its results are compared among each other characterizing an optimization by means ES technique, being the goal the minimization of maximum deflection and minimization of maximum von Mises stress.

Therefore, before the application of the proposed methodology, it was necessary to perform the computational model verification. First, it was verified the computational model applied to the reference plate (see Fig. 2a). To do so, the analytical solution for the central deflection of a clamped plate with no stiffeners is given by [36]

$$w_{\text{central}} = \frac{0.03048 q b^4 \left(1 - \nu^2\right)}{E t^3}, \tag{4}$$

where q is the uniformly distributed transverse load. From Eq. (4) a central deflection of 0.1734 mm was obtained.

Employing the developed computational model, simulating only 1/4 of the plate due to the symmetry boundary conditions, with a converged mesh of 10296 quadrilateral SHELL281 finite elements with size of 7 mm, the central deflection of the plate was 0.1739 mm.

If compared the numerical result with the analytical one, a difference of 0.29% is achieved, verifying the developed computational model.

Next, the verification of the computational model applied to the stiffened plates was performed with a square steel plate, clamped on four sides, with two orthogonal stiffeners (Fig. 4) and subjected to a uniform transversal load of 9.8 kPa; having the following material properties: E = 210 GPa and ν = 0.30. The results of the present study were compared with those presented by Salomon [7].

According to Salomon [7] a variation in the height of the stiffeners h (see Fig. 4) from 10 to 100 mm (with an increment of

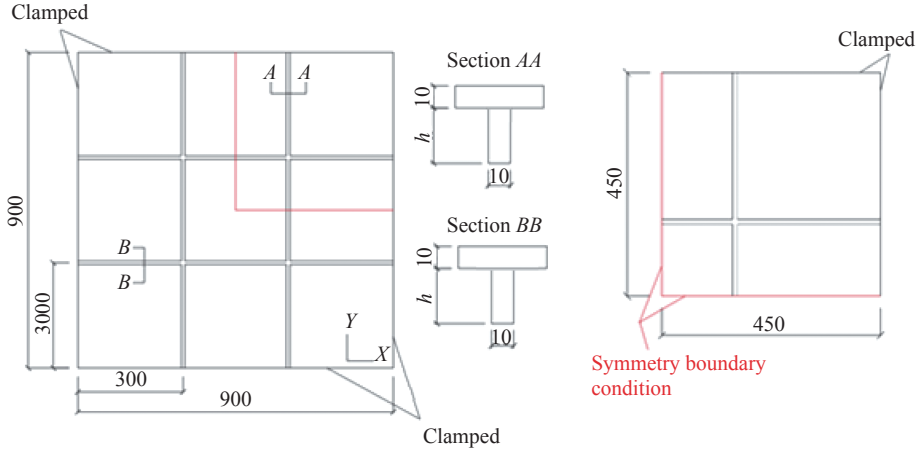

Fig. 4. Square plate with two orthogonal stiffeners (unit: mm)

10 mm) was carried out, being the analysis based on the results of maximum displacement (w) and maximum bending stress of the stiffeners (σ).

So, to reproduce this study a mesh convergence test was developed for the entire plate and for 1/4 of the plate (with symmetry boundary conditions), as can be viewed in Fig. 4. To exemplify, Fig. 5 shows the results for the mesh convergence test for the case with h = 100 mm.

Figure 5a shows that the stabilization of the maximum deflection analysis occurred for the mesh with 2604 elements (element size of 22 mm) in the entire plate. For the plate that employs the symmetry condition, it was used a mesh with 216 elements (element size of 44 mm). Regarding the analysis of the bending stress, Fig. 5b indicates that the stabilization occurred for a mesh with 10416 elements for the entire plate and 2604 elements for the plate with symmetry. In both cases, for the stress analysis, the size of the element was 11 mm.

Mesh convergence test for the other cases (h = 10, 20, 30, 40, 50, 60, 70, 80, and 90 mm) were carried out in a similar manner to that presented in Fig. 5 for the case h = 100 mm. So, the obtained

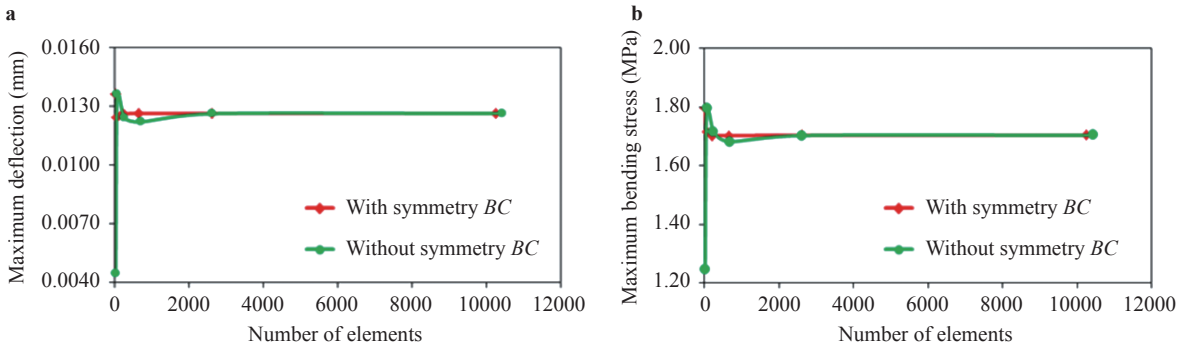

Fig. 5. Mesh convergence test for the case with h = 100 mm. **a** Maximum displacement and **b** maximum bending stress

Table 1 Size of the simulated element for the entire plate and the plate with symmetry

h (mm)	Element size (mm)	Number of elements		w (mm)		σ (MPa)	
		Entire plate	1/4 of the plate	Entire plate	1/4 of the plate	Entire plate	1/4 of the plate
10	9.50	9984	2496	0.3287	0.3287	14.7522	14.7522
20	9.50	10368	2592	0.1860	0.1860	14.1192	14.1192
30	9.75	10137	2688	0.1004	0.1005	10.2734	10.2786
40	9.80	10509	2784	0.0592	0.0592	7.2464	7.2502
50	10.00	9900	2475	0.0387	0.0387	5.2686	5.2686
60	10.25	10260	2565	0.0276	0.0276	3.9757	3.9757
70	10.50	10005	2655	0.0211	0.0212	3.0996	3.1018
80	10.50	10353	2745	0.0171	0.0171	2.4856	2.4874
90	11.00	10080	2520	0.0145	0.0145	2.0399	2.0399
100	11.00	10416	2604	0.0126	0.0126	1.7038	1.7038

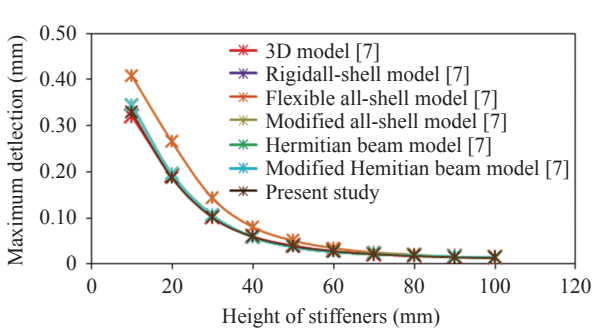

Fig. 6. Computational model verification for maximum deflection

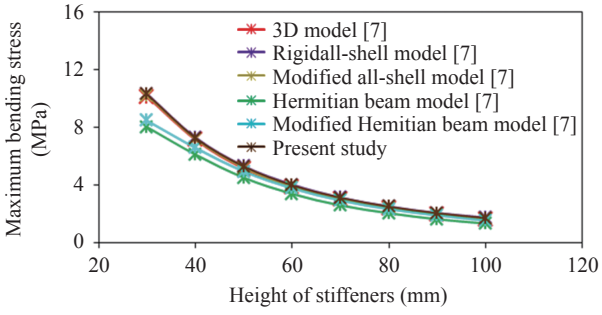

Fig. 7. Computational model verification for maximum bending stress

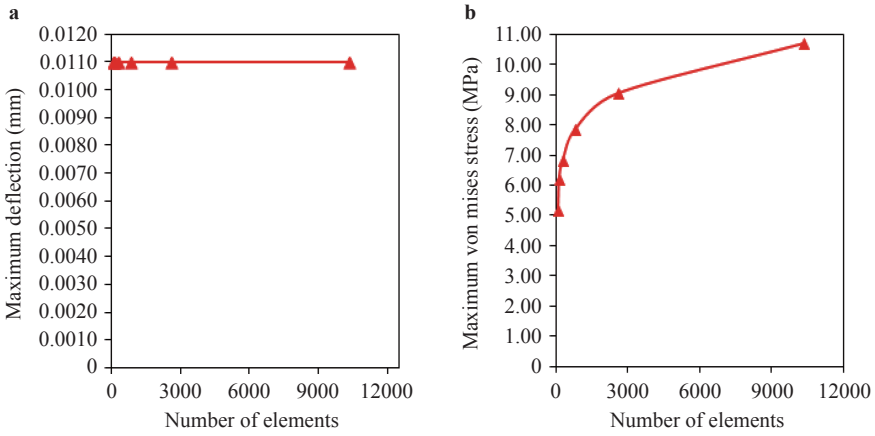

Fig. 8. Mesh convergence test for **a** maximum deflection and **b** von Mises stress of the plate P(6, 6) with $h_s / t_s = 66.3476$ with symmetry

results in all mesh convergence tests are presented in Table 1.

It is important to highlight that, as expected, the converged mesh adopted for each case (see Table 1) was defined by the mesh convergence test related with the maximum bending stress. In addition, also in Table 1, one can observe that the numerical results for both maximum out-of-plane displacement and maximum bending stress considering 1/4 of the plate conduct to very similar values to those obtained with entire plate.

Thereafter, the numerical results obtained by the proposed model with the converged meshes were compared to those presented by Ref. [7], being Figs. 6 and 7 related to maximum deflection and maximum stress, respectively.

Figures 6 and 7 indicate, respectively, that the results of deflection and stress obtained in the present study are in good agreement with the results presented in Ref. [7]. Among the computational models adopted in Ref. [7], the most accurate is the 3D model. Then, using the 3D model as a reference, it was reached a maximum difference for the deflection analysis around 6% and a maximum difference for the stress analysis around 5%, which occurs for the highest values of h (90 and 100 mm). From these comparisons, it is possible to affirm that the developed computational model was adequately verified.

Despite the performed verification, it is well known that the ideal way for the accuracy evaluation of a computational model is by means a validation, i.e., the comparison of its numerical results with experimental data. However, for the present work no adequately experimental cases were found.

From the computational model verifications, the earlier proposed methodology it was applied in a case study. To do so, a mesh convergence test was developed considering the stiffened plate with greater geometric complexity among all configurations of search space, i.e., the plate P(6, 6) with $h_s / t_s = 66.3476$. Figure 8 shows the numerical results for the mesh convergence test concerning the maximum deflection (Fig. 8a) and the maximum von Mises stress (Fig. 8b) analysis for the plate P(6, 6) with $h_s / t_s = 66.3476$. For the deflection analysis it was possible to determine the solution of mesh independence, as can be observed in Fig. 8a. The used mesh required 91 elements with a size of 384 mm. However, for the von Mises stress analysis the results indicated a need for the use of more refined meshes due to the non-stabilization of the test.

Therefore, from Fig. 8 one can observe an excellent mesh

Table 2 Finite element size SHELL281 used in each P(N_{ls}, N_{ts})

P(N_{ls}, N_{ts})	Number of elements	Element size (mm)
P(2, 2)	10206	9.50
P(2, 3)	10398	10.25
P(2, 4)	9948	10.00
P(2, 5)	9900	11.25
P(2, 6)	10512	10.75
P(3, 2)	10128	10.50
P(3, 3)	10472	11.50
P(3, 4)	10124	11.50
P(3, 5)	10254	11.50
P(3, 6)	9970	11.75
P(4, 2)	10314	11.00
P(4, 3)	10564	11.00
P(4, 4)	10550	11.00
P(4, 5)	10080	12.50
P(4, 6)	10446	12.35
P(5, 2)	10035	11.25
P(5, 3)	10218	13.00
P(5, 4)	10488	12.75
P(5, 5)	10062	12.85
P(5, 6)	10287	12.85
P(6, 2)	10290	12.00
P(6, 3)	10374	12.25
P(6, 4)	10350	12.25
P(6, 5)	10044	12.50
P(6, 6)	10332	12.00

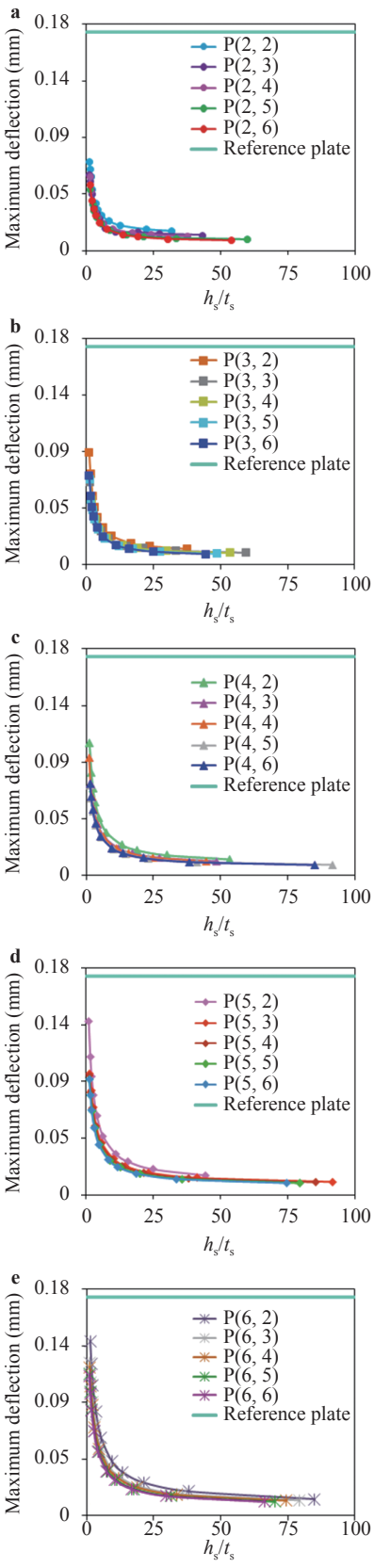

Fig. 9. Variations of the maximum deflection as a function of h_s/t_s for **a** N_{ls}=2, **b** N_{ls}=3, **c** N_{ls}=4, **d** N_{ls}=5, and **e** N_{ls}=6

convergence for the deflection analysis (Fig. 8a); while for the von Mises stress a stabilization trend can be observed (Fig. 8b), but being necessary more refined meshes to obtain the convergence. The ANSYS 18.2 academic version limits the computational modeling to a maximum use of 32000 nodes per simulation. For this reason, the more refined possible mesh was employed for each geometric configuration numerically simulated in this work, as indicated in Table 2. Therefore, the maximum value of the von Mises stress was used only as a means of comparison, and not as definitive value.

Thereafter, employing the verified model, the proposed geometries by means CD were numerically simulated with spatial discretization indicated in Table 2. From the obtained results, scatter plots were generated with maximum deflection (Fig. 9) and maximum von Mises stress (Fig. 10) for each geometric combination P(N_{ls}, N_{ts}) as a function of the degree of freedom h_s/t_s.

Figure 9 indicates that the transformation of 30% of reference plate volume into stiffeners always leads to an improvement over deflection, i.e., all stiffened plates have a smaller maximum deflection than the reference plate. In turn, for the maximum von Mises stress (Fig. 10), it can be noted that there is a specific value of h_s/t_s from which it is possible to obtain a stiffened plate with a superior performance than the reference plate. For instance, in Fig. 10a this h_s/t_s value is approximately 5, having several configurations submitted to smaller stress than reference plate. On the other hand, in Fig. 10e only the plate P(6, 6) with h_s/t_s = 66.3476 reached a stress slightly smaller than reference plate. However, for values of h_s/t_s smaller than these specific magnitudes, there was an increase in the maximum stress and, consequently, a worsening in the stress mechanical behavior if compared with reference plate.

Another observed aspect is that as the value of h_s/t_s increases, the deflection (Fig. 9) and the von Mises stress (Fig. 10) of the stiffened plates decrease. An explanation for this, as previously observed in Ref. [13], is due the increase in the moment of inertia of the cross-section of the new structures formed.

Next, Table 3 shows the best geometric configurations for each P(N_{ls}, N_{ts}), i.e., the stiffened plates that minimized the deflection and von Mises stress of each combination of longitudinal and transverse stiffeners addressed in this study.

Observing Table 3, it was noticed that P(2, 6) with h_s/t_s = 53.4905 has the minimum value for the maximum deflection, being 95.23% smaller than the maximum deflection of reference plate. About the stress analysis, P(2, 5) with h_s/t_s = 59.4087 is the best geometry, achieving a stress reduction of 44.98% if compared with the reference plate.

From Table 3, the influence of N_{ts} over the performance indicators is depicted in Fig. 11. It was inferred that when N_{ts} increases, in a general way, occurs a decrease of the maximum deflection and a decrease of the maximum von Mises of the stiffened plates.

Finally, in Fig. 12 was carried out a qualitative evaluation of the deflected configuration for the reference plate (Fig. 12a), plate P(6, 2) with h_s/t_s = 1.3581 (worst geometry for deflection purpose, in Fig. 12b), and plate P(2, 6) with h_s/t_s = 53.4905 (best geometry for deflection purpose, in Fig. 12c). In a similar way, Fig. 13 shows the von Mises stress distribution of reference plate (Fig. 13a), plate P(6, 3) with h_s/t_s = 1.2790 (worst geometry for the stress purpose, Fig. 13b), and plate P(2, 5) with h_s/t_s =

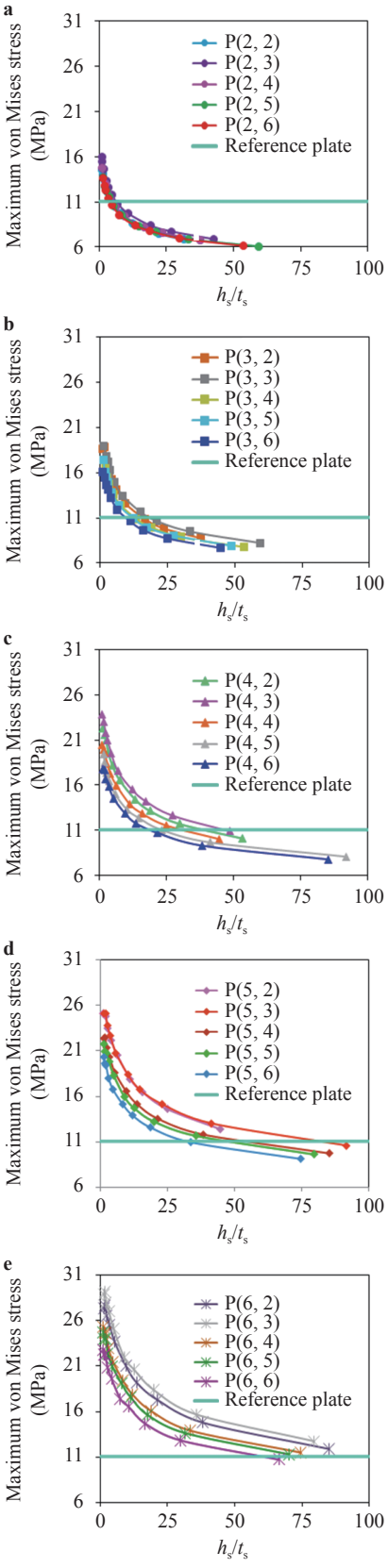

Fig. 10. Variations of the von Mises maximum stress as a function of h_s/t_s for **a** $N_{ls} = 2$, **b** $N_{ls} = 3$, **c** $N_{ls} = 4$, **d** $N_{ls} = 5$, and **e** $N_{ls} = 6$

59.4087 (best geometry for stress purpose, Fig. 13c).

From Fig. 12, the stiffened plate P(6, 2) with h_s/t_s = 1.3581 (Fig. 12b) has a global deflection mechanical behavior quite similar to that of the reference plate (Fig. 12a); while the best plate P(2, 6) has local deflections among the stiffeners. This fact occurs due to the regions confined among stiffeners that behave like small square plates supported in its four edges (due to the high h_s/t_s ratio), allowing the rigidity improvement. This same trend can be observed in Fig. 13, where the best geometry also has an elevated h_s/t_s value and the almost square regions formed by the stiffeners arrangement, allowing the improvement of mechanical resistance.

Based on the presented results, it was possible to determine a time gain in the computational processing of the simulations, because the proposed model reduces the computational domain of the problem and, as a consequence, needs fewer finite elements for their spatial discretization. For example, adopting a quadrilateral SHELL281 finite element with size of 24 mm, the

Table 3 Best geometric configurations for each P(N_{ls}, N_{ts})

Plate	h_s/t_s	w (mm)	σ_{vM} (MPa)
P(2, 2)	31.4176	0.0158	6.8348
P(2, 3)	42.7470	0.0126	6.8799
P(2, 4)	37.4378	0.0115	6.7789
P(2, 5)	59.4087	0.0091	6.0782
P(2, 6)	53.4905	0.0083	6.1451
P(3, 2)	37.3781	0.0128	8.7677
P(3, 3)	59.3771	0.0098	8.2325
P(3, 4)	53.4905	0.0096	7.7748
P(3, 5)	48.6658	0.0089	7.9187
P(3, 6)	44.6394	0.0087	7.6923
P(4, 2)	53.3885	0.0128	10.0742
P(4, 3)	48.6024	0.0114	10.8693
P(4, 4)	44.6038	0.0114	10.0198
P(4, 5)	91.7305	0.0085	8.0793
P(4, 6)	85.2262	0.0084	7.7685
P(5, 2)	44.4975	0.0154	12.3992
P(5, 3)	91.6179	0.0103	10.5903
P(5, 4)	85.1484	0.0101	9.7187
P(5, 5)	79.5323	0.0095	9.5940
P(5, 6)	74.6112	0.0093	9.1071
P(6, 2)	84.9932	0.0132	11.8790
P(6, 3)	79.4138	0.0122	12.7369
P(6, 4)	74.5218	0.0120	11.4844
P(6, 5)	70.1976	0.0112	11.2828
P(6, 6)	66.3476	0.0110	10.7066

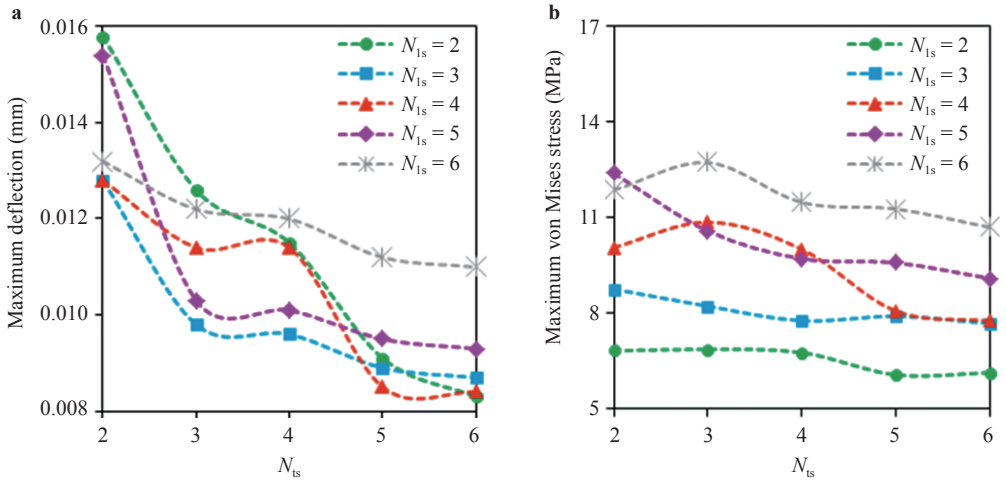

Fig. 11. Variation as a function of N_{ts} of **a** maximum deflection and **b** maximum von Mises stress

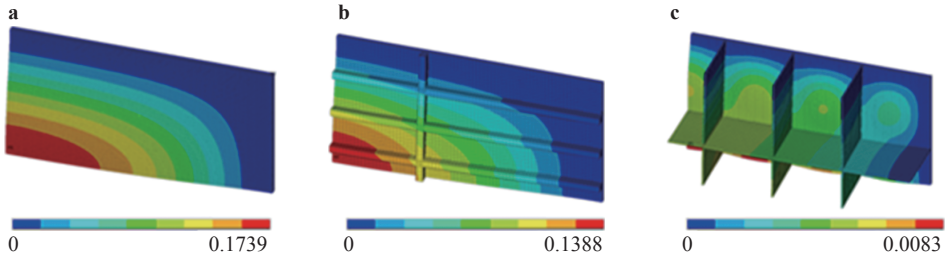

Fig. 12. Deflected configuration of the plates (in mm): **a** reference, **b** P(6, 2), and **c** P(2, 6)

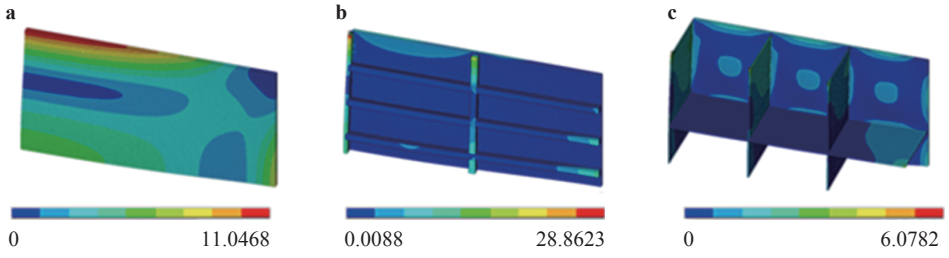

Fig. 13. Stress distribution of the plates (in MPa): **a** reference, **b** P(6, 3), and **c** P(2, 5)

plate P(6, 6) with $h_s/t_s = 66.3476$ showed a reduction in computational processing time of 75.38%, since the plate with symmetry requires only 1.00 s to solve the equations of 2583 elements; while the model that considers the entire plate as computational domain required 4.06 s to solve the equations of 10332 finite elements. Regarding the random access memory (RAM) of the computer allocated to solve these models, the entire plate model used 747.25 MB, while the developed model using symmetry boundary conditions needed only 162.30 MB, demonstrating a reduction of 78.28% in the RAM.

Moreover, the CD method and the Exhaustive Search technique were used in conjunction with the developed computational model aiming to define the best geometric configurations that minimize the deflection and minimize the stress of clamped stiffened steel plates subjected to uniformly distribute transverse load. It has been shown that the transformation of 30% of the volume of a non-stiffened reference plate into longitudinal and transverse stiffeners can results in an improvement of structural mechanical performance. It was also observed that in addition to the number of longitudinal stiffeners N_{ls} and transverse stiffeners N_{ts}, the ratio of stiffener height per stiffener thickness h_s/t_s had a strong influence on the rigidity and resistance of the stiffened plates. For the performed stress analysis, the h_s/t_s variation was the geometric parameter that defined if the stiffened plate achieved or not a superior performance than the reference plate. Regarding the improvement on the deflections, all stiffened plates reached a smaller deflection than the reference plate; with the increasing of the h_s/t_s ratio conducting to the deflection reduction. Among all search space configurations and considering the proximity for the deflections and stress results, it is possible to indicate the stiffened plates P(2, 5) and P(2, 6) as the optimized geometries for the improvement of mechanical behavior.

Finally, the study of different geometric configurations with

the same volume of material proved that the simple increase in the number of stiffeners does not always imply in the mechanical behavior improvement of stiffened plates, evidencing the importance of the geometric evaluation in this type of structural component.

Acknowledgement

This study was financed in part by the CAPES (Coordination for the Improvement of Higher Education Personnel), finance code 001. The authors also thank FAPERGS (Foundation for Research Support of the State of Rio Grande do Sul), CNPq (Brazilian National Council for Scientific and Technological Development) and the Italian Minister of Foreign Affairs and International Cooperation (MAECI), as part of the "Two Seats for a Solar Car" international project.

References

[1] G. Rama, D. Marinkovic, M. Zehn, A three-node shell element based on the discrete shear gap and assumed natural deviatoric strain approaches, Journal of the Brazilian Society of Mechanical Sciences and Engineering 40 (2018) 356.

[2] K. Saravanakumar, B.S. Lakshminarayanan, V. Arumugam, et al., Quasi-static indentation behavior of GFRP with milled glass fiber filler monitored by acoustic emission, Facta Universitatis - Series Mechanical Engineering 17 (2019) 425–443.

[3] A. Pagani, E. Carrera, Large-deflection and post-buckling analyses of laminated composite beams by Carrera Unified Formulation, Composite Structures 170 (2017) 40–52.

[4] D. Marinković, G. Rama, M. Zehn, Abaqus implementation of a corotational piezoelectric 3-node shell element with drilling degree of freedom, Facta Universitatis, Series: Mechanical Engineering 17 (2019) 269–283.

[5] R. Szilard, Theories and Applications of Plate Analysis: Classical Numerical and Engineering Methods, John Wiley & Sons, Inc., Hoboken, New Jersey (2004).

[6] N.E. Shanmugam, C.M. Wang, Analysis and Design of Plated Structures, Woodhead Publishing Limited, Abington Hall, Cambridge, England (2006).

[7] A. Salomon, An evaluation of finite element models of stiffened plates, [Master's Thesis], Massachusetts Institute of Technology (2001).

[8] J.R. O'Leary, I. Harari, Finite element analysis of stiffened plates, Computers & Structures 21 (1985) 973–985.

[9] E.J. Sapountzakis, J.T. Katsikadelis, Analysis of plates reinforced with beams, Computational Mechanics 26 (2000) 66–74.

[10] L. Banai, O. Pedatzur, Computer implementation of an orthotropic plate model for quick estimation of the maximum deflection of stiffened plates, Ships and Offshore Structures 1 (2010) 323–333.

[11] E.J. Sapountzakis, V.G. Mokos, An improvement model for the analysis of plates stiffened by parallel beams with deformable connection, Computers & Structures 86 (2008) 2166–2181.

[12] K. Bhaskar, A. Pydah, An elasticity approach for simply-supported isotropic and orthotropic stiffened plates, International Journal of Mechanical Sciences 89 (2014) 21–30.

[13] G. Troina, M. Cunha, V. Pinto, et al., Computational modeling and constructal design theory applied to the geometric optimization of thin steel plates with stiffeners subjected to uniform transverse load, Metals 10 (2020) 220.

[14] A. Bejan, S. Lorente, Design with Constructal Theory, Wiley, Hoboken (2008).

[15] A. Bejan, interviewed by A.W. Kosner, "Freedom is good for design," How to use constructal theory to liberate any flow system, Forbes (2012).

[16] A. Bejan, The Physics of Life: the Evolution of Everything, St. Martin Press, New York (2016).

[17] A. Bejan, S. Lorente, The constructal law of design and evolution in nature , Philosophical Transactions of the Royal Society B 365 (2010) 1335–1347.

[18] A. Bejan, Advanced Engineering Thermodynamics, Wiley, Hoboken (2006).

[19] A.H. Reis, Constructal view of scaling laws of river basins, Geomorphology 78 (2006) 201–206.

[20] E. Cetkin, S. Lorente, A. Bejan, Natural constructal emergence of vascular design with turbulent flow, Journal of Applied Physics 107 (2010) 114901.

[21] L.A.O. Rocha, G.C. Montanari, E.D. Dos Santos, et al., Constructal Design applied to the study of cavities into a solid conducting wall, Thermal Engineering 60 (2007) 41–47.

[22] C. Biserni, L.A.O. Rocha, G. Stanescu, et al., Constructal H-shaped cavities according to Bejan's theory, International Journal of Heat and Mass Transfer 50 (2007) 2132–2138.

[23] G. Lorenzini, L.A.O. Rocha, Geometric optimization of T-Y-shaped cavity according to constructal design, International Journal of Heat and Mass Transfer 52 (2009) 4683–4688.

[24] G.M. Barros, G. Lorenzini, L.A. Isoldi, et al., Influence of mixed convection laminar flows on the geometrical, International Journal of Heat and Mass Transfer 114 (2017) 1188–1200.

[25] S. Lorente, J. Lee, A. Bejan, The "flow of stresses" concept: the analogy between mechanical strength and heat convection, International Journal of Heat and Mass Transfer 53 (2000) 2963–2968.

[26] L.A. Isoldi, M.V. Real, A.L.G. Correia, et al., The flow of stresses: constructal design of perforated plates subjected to tension or buckling, in: L.A.O. Rocha, S. Lorente, A. Bejan (Eds.), Constructal Law and the Unifying Principle of Design - Understanding Complex Systems, Springer, New York (2013) 195–218.

[27] P. Mardanpour, E. Izadpanahi, S. Rastkar, et al., Constructal design of aircraft: Flow of stresses and aeroelastic stability, AIAA Journal 57 (2019) 1–13.

[28] E. Izadpanahi, M. Moshtaghzadeh, H.R. Radnezhad et al., Constructal approach to design of wing cross-section for better flow of stresses, AIAA Scitech (2020). doi: 10.2514/6.2020-0275

[29] D. Helbig, C.C.C. Da Silva, M.V. Real, et al., Study about buckling phenomenon in perforated thin steel plates employing computational modeling and Constructal design method, Latin American Journal of Solids and Structures 13 (2016) 1912–1936.

[30] C.C.C. Da Silva, D. Helbig, M.L. Cunha, et al., Numerical buckling analysis of thin steel plates with centered hexagonal perforation through Constructal design method, Journal of the Brazilian Society of Mechanical Sciences and Engineering 41 (2019) 309.

[31] J.P.S. Lima, L.A.O. Rocha, E.D. Dos Santos, et al., Constructal design and numerical modeling applied to stiffened steel plates submitted to elasto-plastic buckling, Proceedings of the Romanian Academy Series A-Mathematics Physics Technical Sciences Information Science, 19 (2018) 195–200.

[32] J.P.S. Lima, M.L. Cunha, E.D. Dos Santos, et al., Constructal design for the ultimate buckling stress improvement of stiffened plates submitted to uniaxial compressive load, Engineering Structures 203 (2020) 109883.

[33] J. De Queiroz, M. Cunha, A. Pavlovic, et al., Geometric evaluation of stiffened steel plates subjected to transverse loading for naval and offshore applications, Journal of Marine Science and Engineering 7 (2019) 7–18.

[34] ANSYS, Inc. ANSYS® Academic Research Mechanical, Release 18.2, Help System, Coupled Field Analysis Guide (2017).

[35] C. Bernuzzi, B. Cordova, Structural Steel Design to Eurocode 3 and AISC Specifications, John Wiley & Sons, Ltd, Oxford (2016).

[36] S. Timoshenko, S. Woinowsky-Krieger, Theory of Plates and Shells, McGraw Hill, New York (1959).